

Excitation of gigahertz magnetoelastic waves in dysprosium films: Field dependence

S. C. Hart, J. G. Sylvester, and H. A. Blackstead

Department of Physics, University of Notre Dame, Notre Dame, Indiana 46556

(Received 15 August 1977)

The excitation of transverse-magnetoelastic waves in polycrystalline dysprosium films, with a static magnetic field applied normal to the film, has been observed using a pulse-echo technique. The "phononlike" excitations propagate parallel to the film normal. For the same experimental configuration, microwave absorption data show a very broad peak with maximum absorption occurring at an applied field of approximately $4\pi M$. The experiments were carried out at 5.7 and 9.0 GHz, and pulse-echo signals were observed at both frequencies from 4.2 to 70 K. The observed echo-signal intensity, field dependence, mode, and frequency are shown to be in excellent agreement with calculations based on a coupled-mode model; the transition-rate calculations also describe the absorption line shape for H_{applied} greater than the demagnetizing field, $4\pi M$. Furthermore, the data are consistent with results obtained using another technique.

I. INTRODUCTION

Conventional microwave resonance investigations¹⁻³ on dysprosium have stimulated much interest, and, as a result, several explanations have been proposed.⁴⁻¹⁰ In light of spin-phonon spectrometer results¹¹ and conventional pulse-echo studies,¹² it appears that the correct approach is to treat Dy as a coupled magnetoelastic system in which the normal modes of oscillation are of mixed magnetic and elastic character. Using such a description, and employing time-dependent perturbation theory, it has been possible to predict phonon signal intensities observed with a spin-phonon spectrometer to within a factor of 2.¹¹ The same approach is also found to describe the mode, magnetic-field dependence, and signal intensity correctly for signals observed with a pulse-echo spectrometer; in addition, the shape of the microwave absorption envelope is predicted.

II. THEORY

The normal-mode analysis for dysprosium, treating the coupled magnon-phonon modes, and the development of the time-dependent perturbation theory appropriate to transverse-magnetoelastic wave excitation, has been given elsewhere¹¹; only the principal results will be reproduced here. Assuming coupling between the magnon and one transverse-phonon mode, the transverse-acoustical power generated in a polycrystalline film can be approximated by¹¹

$$P_{\text{acous}} = \left(\frac{4}{15}\right)^2 (2\omega_0 d C_1^2) |f(q)|^2 |S_{14}(q) + S_{24}(q)|^2 \times [S_{33}(q)S_{44}(q)] / \hbar V_{q,T}, \tag{1}$$

where

$$f(q) = \frac{1 - \exp[id(q + 1/\Delta) - d/\Delta]}{d[1/\Delta - i(q + 1/\Delta)]}, \tag{2}$$

$$C_1 = g \mu_B H_{\text{rf}}^0 (\frac{1}{2} JN)^{1/2}. \tag{3}$$

$V_{q,T}$ is the transverse-phonon velocity, d is the film thickness, and Δ is the usual microwave skin depth. For a particular value of applied field, $|\vec{q}|$ is determined by the solution of $\omega_0 = \Omega^-(q)$. Here Ω^- is the angular frequency of the "phononlike" magnetoelastic mode, and the wave-vector direction is parallel to the film normal. S_{ij} are elements of the transformation matrix S which diagonalizes the Hamiltonian, and H_{rf}^0 is the amplitude of the rf perturbation field at the sample. For the 5.7-GHz coaxial cavity, H_{rf}^0 is given by^{13,14}

$$H_{\text{rf}}^0 = [4PQ / 1500r_i^2 \ln(r_o/r_i)]^{1/2} \text{ Oe}. \tag{4}$$

Here P is the input power in watts, and r_i and r_o are the inner and outer radii of the cavity, in cm. For the rectangular cavity used at 9 GHz, H_{rf}^0 is given by^{13,14}

$$H_{\text{rf}}^0 = (16\pi P Q \lambda^3 / 1500ab\lambda_g^3)^{1/2} \text{ Oe}, \tag{5}$$

where a and b are the inner dimensions, in cm, of the wave guide used, and λ and λ_g are the wavelengths of the microwave radiation in free space and in the wave guide, respectively. For both cavities the cavity quality factor Q was measured.

To compute the pulse-echo signal intensity, it is assumed that the conversion efficiency of the inverse process (phonon → photon) is the same as that of the original process (photon → phonon) and is given by $P_{\text{acous}}/P_{\text{in}}$. Furthermore, the acoustical energy returning to the sample in the first echo is given by $P_{\text{acous}} L T_1 T_2$. Here L is the transmission factor of the delay line which at low temperatures is approximately unity. T_1 and T_2 are the transmission coefficients for acoustical coupling from the sample into the delay line, and for transmission back into the film from the substrate, respectively. The product $T_1 T_2$ is given by

$$T_1 T_2 = 4 \left(2 + \frac{\rho_f V_f}{\rho_s V_s} + \frac{\rho_s V_s}{\rho_f V_f} \right)^{-1}, \quad (6)$$

where ρ is the density, V is the phonon group velocity in the material, and the subscripts f and s refer to the film and substrate, respectively. Therefore, the echo-signal intensity is given by¹⁵:

$$P_{\text{echo}} = \left(\frac{4}{15} \right)^4 |f(q)|^4 |S_{14}(q) + S_{24}(q)|^4 (g \mu_B H_{\text{rf}}^0)^4 \times \left(\frac{64 q^2 d^2 J^2 N^2 |S_{33}(q) S_{44}(q)|^2}{P_{\text{in}} \hbar^2 [2 + (\rho_f V_f / \rho_s V_s) + (\rho_s V_s / \rho_f V_f)]} \right), \quad (7)$$

where P_{in} is the input power adjusted to include the various system insertion losses. For all measurements, the cavity coupling factor was adjusted for maximum power transfer. From Ref. 11, the total microwave power absorption is given by

$$P_{\text{abs}} = \left(\frac{4}{15} \right)^2 (2 \omega_0 d C_1^2) |f(q)|^2 \times |S_{14}(q) + S_{24}(q)|^2 / \hbar V_{q,T}. \quad (8)$$

III. SAMPLE PREPARATION AND EXPERIMENTAL PROCEDURE

The samples for this investigation were prepared by evaporating high-purity (99.9%) Dy, under high vacuum, $P < 10^{-7}$ Torr, onto one end of an ultrasonic delay line, and then overlaying the Dy

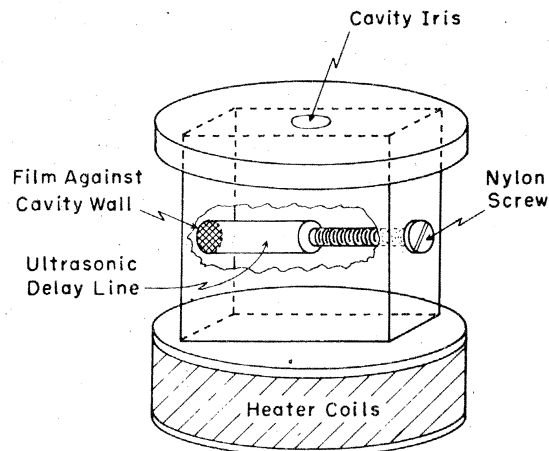


FIG. 1. Cutaway view of a rectangular TE_{101} mode cavity showing the position of the delay line and the sample.

film with 5 kÅ of SiO to protect it from oxidation. The delay lines, C-axis sapphire single-crystal cylinders, 15 mm long by 3.17 mm in diameter, have both ends polished optically flat and parallel within 0.1 arcsec. The delay line was then placed in a microwave resonant cavity such that the film was located in a region of intense rf magnetic field, see Fig. 1.

A pulse-echo spectrometer, described in Fig. 2, was employed to determine the polarization

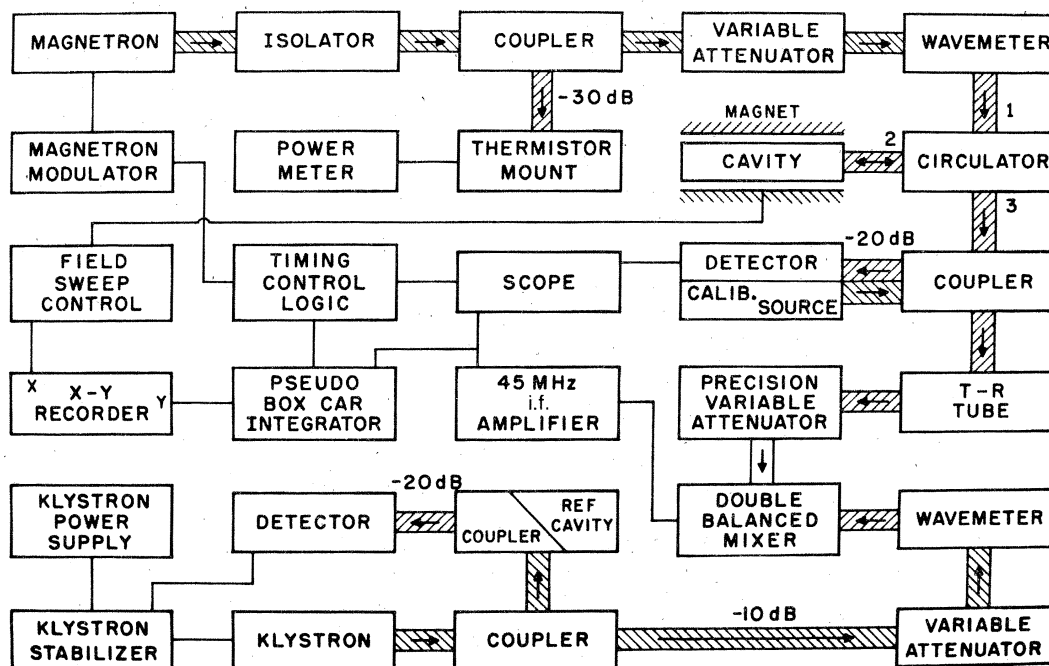


FIG. 2. Block diagram of the pulse-echo spectrometer. The microwave connections are shaded, with the arrows indicating the microwave propagation direction.

and measure the echo-signal intensity as a function of the applied magnetic field. A magnetron provides rf pulses with a peak power of 1 kW with a 1- μ sec duration which are coupled into the cavity to perturb the magnetic system and excite magnetoelastic waves which propagate parallel to the film normal. These magnetoelastic waves are partially coupled into the delay line where they propagate as acoustical waves. The wave packet travels to the free end of the rod, is reflected, and returns to the sample in a time τ , which is determined by the properties of delay line material and the delay line length. When this acoustical pulse returns to the sample, a percentage of acoustical energy, as determined by the sample to delay line acoustical transmission coefficient, will be coupled back into the sample. The remainder of the energy will be reflected, propagate to the free end of the delay line, return to the sample, etc. The energy which was coupled back into the sample will, by the inverse process which excited the original magnetoelastic wave, generate a very weak microwave "echo" pulse, which is then detected using a superheterodyne receiver. In order to measure the echo signals, nominal 1- μ sec pulses, the output of the i.f. amplifier is sampled using a fast sample and hold amplifier gated at twice the magnetron repetition rate (1 kHz). First, the sum of the signal and the noise is sampled, and approximately 500 μ sec later, after the echo train has decayed away, the noise is sampled. This technique¹⁶ produces a square wave with an amplitude proportional to the echo signal which is then measured using a lock-in amplifier.

In normal operation, the cavity containing the sample is stabilized to the desired temperature and the magnetic field is swept through the region of interest. During each sweep, the field-dependent signal output of the lock-in amplifier is digitized and stored in a signal-averager system.

To calibrate the signal recovery system response, a low-level pulse of known intensity is injected into the receiver and recorded. The set of calibration points is used to interpolate the raw pulse-echo signals, thereby determining an absolute power level for the signal as a function of applied field.

IV. RESULTS AND CONCLUSIONS

Using typical experimental values¹⁷⁻²¹ for various parameters, pulse-echo and microwave absorption signals were calculated as a function of applied magnetic field from 38 to 90 kOe. No attempt was made to compute signals for applied fields less than the demagnetizing field $4\pi M$, since the films are not saturated. The results of these

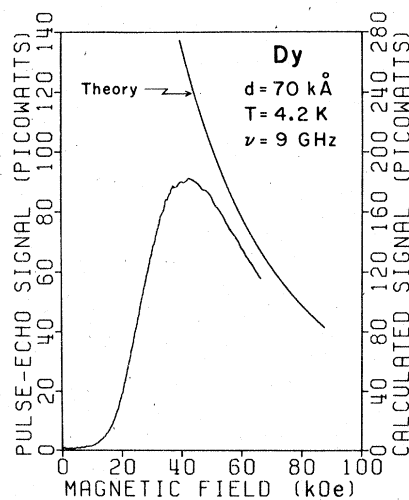


FIG. 3. Typical pulse-echo spectrometer signal and computer signal at 9 GHz as a function of applied field strength for a 70-kÅ polycrystalline Dy film with the static magnetic field applied normal to the film. The left-hand scale refers to the experimental values and the scale on the right corresponds to the signals computed from the coupled-mode model.

calculations and typical experimental data are shown in Figs. 3 and 4, for the pulse-echo signals, and Figs. 5 and 6, for the microwave absorption signals. The agreement between theory and the experimental results is excellent, both for the pulse-echo signal intensity, and for the magnetic-field dependence of the pulse-echo and mi-

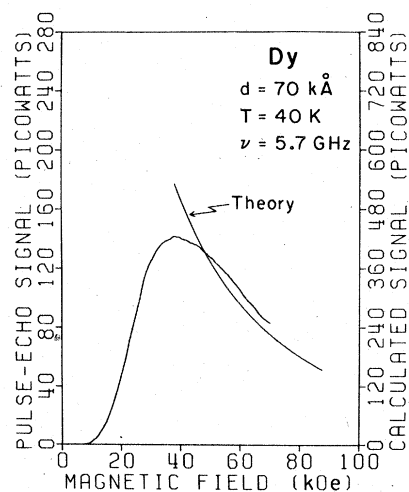


FIG. 4. Typical pulse-echo spectrometer signal and computed signal at 5.7 GHz as a function of applied field strength for a 70 kÅ polycrystalline Dy film with the static magnetic field applied normal to the film. The left-hand scale refers to the experimental values, and the scale on the right corresponds to the signals computed according to the coupled-mode model.

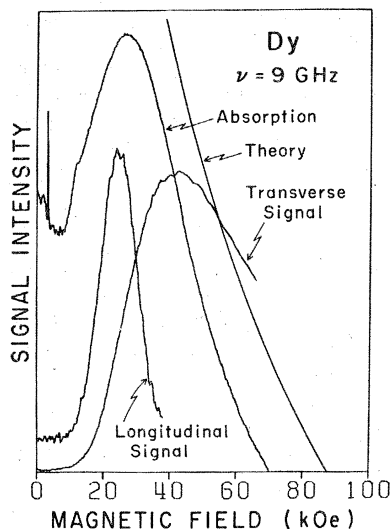


FIG. 5. Computed and experimental microwave absorption signals at 9 GHz. Since the absorption signal represents the envelope of all absorption processes, the observed longitudinal and transverse pulse-echo spectrometer signals are also shown to suggest how the absorbed energy is distributed in the normal modes.

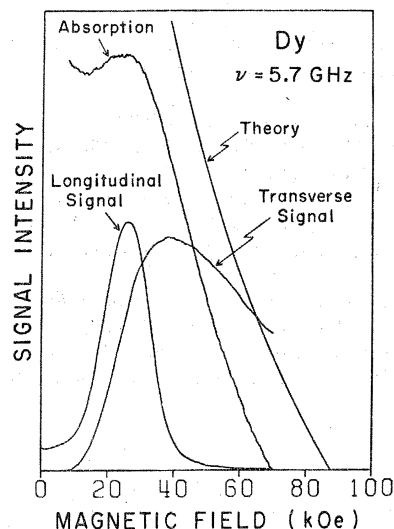


FIG. 6. Computed and experimental microwave absorption signals at 5.7 GHz. Since the absorption signal represents the envelope of all absorption processes, the observed longitudinal and transverse pulse-echo spectrometer signals are also shown to suggest how the observed energy is distributed in the normal modes.

crowave absorption signals. As the applied static magnetic field is increased, the magnon energy gap increases, and this leads to a decrease in the relative coupling between the magnon and transverse-phonon-dispersion curve branches at low (~ 10 GHz) frequencies. Thus, as the "phononlike" dispersion curve branch becomes less magnetic in character, the excitation of "phononlike" magnetoelastic waves by an rf magnetic field is diminished.

Longitudinal pulse-echo signals have been observed for applied fields less than the demagnetizing field $4\pi M$, and while the model is not valid in this region, typical signals have been illustrated in Figs. 5 and 6 to demonstrate one source of energy absorption in this field range.

The results of spin-phonon spectrometer studies,¹¹ which show that magnetoelastic wave generation occurs at the driving frequency, and in which the observed signal intensities agree with the coupled-mode theory to within a factor of 2, are also consistent with the results of this study. It is concluded, from these results, and from the

results of spin-phonon spectrometer studies, that the coupled normal-mode approach used by Wang, O'Donnell and Blackstead¹¹ provides the correct description of the microwave frequency magnetoelastic properties of dysprosium.

The temperature dependence of the magnetoelastic echo-signals was studied briefly from 4.2 to 70 K, and signals were observable over this temperature range. However, the analysis is complicated by the temperature-dependent phonon attenuation in the delay line²² and the data are not sufficiently reliable to draw any conclusions relating to the temperature dependence of the relative magnetoelastic coupling, the magnon energy gap, etc.

ACKNOWLEDGMENTS

This work was supported in part by a grant from the Research Corp. and by NSF Grant No. DMR 73-02551-A01.

¹T. K. Wagner and J. L. Stanford, *Phys. Rev. B* **5**, 1876 (1972).

²D. M. S. Bagguley and J. Liesegang, *J. Appl. Phys.* **37**, 1220 (1966).

³F. C. Rossol and R. V. Jones, *J. Appl. Phys.* **37**, 1227 (1966).

⁴E. A. Turov and V. G. Shavrov, *Fiz. Tverd. Tela* **1**, 217 (1965) [*Sov. Phys.-Solid State* **1**, 166 (1965)].

⁵B. R. Cooper, *Phys. Rev.* **169**, 281 (1968).

⁶D. T. Vigren and S. H. Liu, *Phys. Rev. B* **5**, 2719 (1972).

⁷B. W. Southern and D. A. Goodings, *Phys. Rev. B* **7**,

- 2028 (1973).
- ⁸H. Chow and F. Keffer, *Phys. Rev. B* 7, 2028 (1973).
- ⁹D. T. Vigen and S. H. Liu, *Phys. Rev. Lett.* 27, 674 (1971).
- ¹⁰S. H. Liu, *Int. J. Magn.* 3, 327 (1972).
- ¹¹J. T. Wang, M. O'Donnell, and H. A. Blackstead, *Phys. Rev. B* 13, 2044 (1976).
- ¹²M. P. Maley, P. L. Donoho, and H. A. Blackstead, *J. Appl. Phys.* 37, 1006 (1966).
- ¹³C. P. Poole, Jr., *Electron Spin Resonance* (Wiley, New York, 1967), Chap. 8.
- ¹⁴Theodore Moreno, *Microwave Transmission Design Data* (Dover, New York, 1958), Chap. 1-4.
- ¹⁵J. D. Achenback, *Wave Propagation in Elastic Solids* (North-Holland, Amsterdam, 1973), Chap. 1.
- ¹⁶H. C. Meyer, A. C. Daniel, and P. L. Donoho, *Rev. Sci. Instrum.* 37, 1262 (1966).
- ¹⁷R. M. Nicklow, N. Wakabayashi, M. K. Wilkinson, and R. E. Reed, *Phys. Rev. Lett.* 26, 140 (1971).
- ¹⁸D. R. Behrendt, S. Legvold, and F. H. Spedding, *Phys. Rev.* 109, 1544 (1958).
- ¹⁹J. J. Rhyne and A. E. Clark, *J. Appl. Phys.* 38, 1379 (1967).
- ²⁰A. E. Clark, B. F. DeSavage, and R. Bozorth, *Phys. Rev.* 138, A216 (1965).
- ²¹S. Legvold, J. Alstad, and J. Rhyne, *Phys. Rev. Lett.* 10, 509 (1963).
- ²²R. Truell, C. Elbaum, and B. B. Chick, *Ultrasonic Measurements in Solid State Physics* (Academic, New York, 1969), Chap. 3.